RESEARCH PAPER

Statistical Optimization and Physicochemical Characterization of Octenidine Dihydrochloride-Loaded PLGA Nanoparticles: In Vitro Release Kinetics and Mechanistic Insights

Koushik Narayan Sarma[1], Chandra Shekar Thalluri[1*]

[1] Faculty of Pharmaceutical Science, Assam down town University, Guwahati, Assam - 781026, India

[*] **Corresponding Author:** Dr. Chandra Shekar Thalluri. Email: chandu6716@gmail.com

ABSTRACT

This work was designed to develop and optimize PLGA nanoparticles loaded with Octenidine Dihydrochloride utilizing Box–Behnken design to explore the physicochemical properties and drug-release profile so that they may be useful for wound healing. A total of 18 formulations with varying polymer concentration, homogenization speed, and sonication time were prepared. The statistical model revealed that the formulation variables have significant effects on mean particle sizes ($R^2 = 0.9749$), entrapment efficiency ($R^2 = 0.9180$), and drug loading ($R^2 = 0.9256$). The optimized nano systems exhibited all the characteristics satisfying a particle size of 237.4 nm, low polydispersity (0.296) indicating uniform distribution, and zeta potential of −12.2 mV, which could be safely considered as moderately stable. The high entrapment efficiency (81.08 ± 1.19%) and drug loading capacity (11.99 ± 0.71%) further characterize the nanoparticles as skillful drug carriers. FT-IR and DSC studies indicated lack of any chemical incompatibility between the drug and PLGA and indicate successful molecular dispersion of drug in the polymer bulk. With regard to in vitro drug release studies, we observed a biphasic release pattern with 20.2% release in the initial burst after 1 h followed by sustained release leading up to 94.3% after 24 h. The kinetic modelling implies diffusion-controlled release, and thus best explained by the Korsmeyer-Peppas model ($R^2 = 0.982$, $n = 0.509$). The optimized nano-system showed total control over the drug release, with great efficiency in encapsulation, favourable physicochemical characters standing as a preferred sustained release platform for wound healing applications.

Keywords: Octenidine Dihydrochloride, PLGA Nanoparticles, Controlled Drug Release, Box–Behnken Design (BBD), Nanoparticle-Based Drug Delivery.

How to cite this article: Sarma KN, Thalluri CS. Statistical Optimization and Physicochemical Characterization of Octenidine Dihydrochloride-Loaded PLGA Nanoparticles: In Vitro Release Kinetics and Mechanistic Insights. Int J Drug Deliv Technol. 2026;16(24s): 1054-1064. DOI: 10.25258/ijddt.16.24s.126

Source of support: Nil.

Conflict of interest: None

INTRODUCTION

The development of controlled release drug delivery systems (DDS) has significantly contributed to the field of pharmacy, particularly where the goal is to increase the efficacy of treatment, lower the side effects, and enhance patients' cooperation. Among the systems of various materials proposed for DDS, Poly (lactic-co-glycolic acid) PLGA nanoparticles have shown great promise with regard to their biodegradability, biocompatibility, and diverse capacities for drug encapsulation[1]. The delivery system based on PLGA nanoparticles is quite innovative and has been reported to deliver several types of drugs - both hydrophobic and hydrophilic agents - positioning PLGA nanoparticles as suitable candidates with a wide range of therapeutic applications in various diseases, such as cancer, cardiovascular diseases, infectious diseases[2].

Octenidine dihydrochloride is a broad-spectrum antimicrobial agent mainly applied in various clinical practices like wound healing, skin antisepsis, and treatment of mucosal infections[3]. However, poor solubility of Octenidine Dihydrochloride considerably limits its practical application with poor bioavailability and consequent lack in therapeutic efficacy[4]. Formulation of Octenidine Dihydrochloride as a nanoparticulate drug delivery system can quickly eliminate its drawbacks for sustained release, increased stability, and improved antibacterial activity at target sites[5].

During recent years, various studies have investigated different strategies for the preparation of Octenidine Dihydrochloride-loaded nanoparticles in order to improve its therapeutic efficiency. There have been numerous medical trials wherein antimicrobial agents, and consequently Octenidine Dihydrochloride, were

encapsulated into PLGA nanoparticles[6]. These preparations would not only make the drug more soluble but would also lead to a more controlled release form, which is highly required to maintain therapeutic concentrations spanning an extended period yet keep the adverse side effects to a minimum[7]. One great challenge lies in the elucidation of the release mechanism and kinetics of drug release from these systems, which are very crucial steps in maximizing the therapeutic potential of these nanocarriers[8].

Several factors determine the kinetic release behaviour of drug-loaded nanoparticles, such as polymer nature, polymer-drug interactions, and physical characteristics of the nanoparticles. These details are crucial to optimize the drug release profile and achieve sustained and controlled Octenidine Dihydrochloride delivery[9]. Several possible mathematical models can be used for explaining the drug release behaviour of drug-loaded nanoparticles, which may include Higuchi model, Korsmeyer-Peppas model, and zero-order kinetics. The models divulge on the release mechanism of drug diffusion from the polymer matrix, as well as factors governing the diffusion process[10].

The aim of this study was to optimize the formulation of Octenidine Dihydrochloride-loaded PLGA nanoparticles by way of a statistical approach and characterize the resulting system with respect to physicochemical properties. The kinetics of in vitro release of the nanoparticulate systems will be studied to be able to elucidate the release mechanisms. This study, however, could well advance our knowledge related to the carrying of Octenidine Dihydrochloride by PLGA nanocarriers in a controlled manner, tackling the limitations hindering its clinical viability.

Basically, the present research, through the formulations of nanoparticles and a study of the mechanisms of release, contributes to the growing knowledge of the use of PLGA nanoparticles in drug delivery, which mainly focus in the antimicrobial area. The results of this study have the expected effects in the future of Octenidine Dihydrochloride therapy and the possible enlargement of the applications of PLGA nanoparticles in any way of drug delivery.

MATERIALS AND METHOD:

Materials: Octenidine Dihydrochloride is purchased from B.L. Chemical Products, Mumbai, Maharashtra; Poly (lactic-co-glycolic acid) (PLGA) is purchased from Yarrow Chem Products in Mumbai, Maharashtra; Dimethyl sulfoxide (DMSO) and Polyvinyl alcohol (PVA) were purchased from Sisco Research Laboratories Pvt. Ltd. Mumbai, Maharashtra. The active pharmaceutical ingredient and all other chemicals which are used in this study were of analytical grade.

Method:

Preparation and Optimization of Octenidine Dihydrochloride: The polymeric nano encapsulated Octenidine Dihydrochloride was then produced utilizing the solvent-evaporation method based on an oil-in-water (o/w) emulsion. The polymer, i.e., previously dissolved in a 1% solvent at diverse rates, was added to Octenidine Dihydrochloride so that a homogenization could begin for one minute using a High-Speed Homogenizer. Emulsification was undertaken in a water phase of polyvinyl alcohol (PVA) and homogenized for a few minutes using a High-Speed Homogenizer. Thereafter, probe sonication was carried out in an ice-water bath. Finally, the emulsion was kept magnetically stirring at 1500 rpm for 5 hours to help evaporation of the solvent. Following the evaporation process, the nanoparticles will be collected by centrifuging at different rates at 4 °C, washed with water to remove excess PVA and PVA-bound drug, then lyophilized and stored for future studies at 5–8 °C[11].

To optimize the nanoparticles formulation, Design Expert software (Version 13) was employed. Using a regular (control) ratio between the polymer drug and stabilizer, the polymer ratio and two designated process parameters of homogenizer speed and sonicate time. The software executed 18 unique runs, whereby all the experiments were run, and three responses, which included particle size, entrapment efficiency, and drug loading capacity, were considered.

Table 1: Formulation of Nano particle by Box-Behnken Design (BBD)

Run	Factors		
	A: Polymer Concentration (%)	B: Homogenization Speed (RPM)	C: Sonication Time (Min)
1	5	10000	5
2	2.75	10000	3
3	2.75	10000	7
4	2.75	20000	3
5	0.5	10000	5
6	2.75	15000	5
7	2.75	15000	5
8	2.75	15000	5
9	0.5	15000	3
10	2.75	15000	5
11	5	15000	3
12	5	15000	7
13	2.75	15000	5

14	5	20000	5
15	2.75	20000	7
16	2.75	15000	5
17	0.5	15000	7
18	0.5	20000	5

Characterization of Optimized Octenidine Dihydrochloride Loaded Nanoparticle

Particle Size and PDI

The particle diffraction analyzer based on photon-correlation spectroscopy simultaneously measured particle size and polydispersity index (PDI) from a Dynamic Light Scattering (DLS) system. Essentially, the technique quantifies particle diffusion from fluctuation in scattered light caused by Brownian motion and converts the diffusion coefficient into hydrodynamic diameter using the Stokes–Einstein equation. The sample was fed into the particle sizer, which was diluted first with filtered dispersion media, so as to achieve acceptable count rates and a subsequent decrease in any multiple scattering effect; and the sample filled the cuvette in a clean area equilibrated for 25 ± 0.5°C before running the analysis. Three replications were made for each sample, each test result averaged and obtained. The obtained average particle-size measurement as z-average hydrodynamic diameter was used to show the extent of particle size dispersion from the solution; and PDI was attained from cumulant analysis of the autocorrelation function as a measure of width of the size distribution and dispersion uniformity[12].

Particle Charge (Zeta Potential)

The electrophoretic light scattering method can be deployed to measure the zeta potential with the help of dynamic light scattering (DLS) for the purpose of establishing the surface charge of particles being synthesized. A Malvern Zeta sizer Nano series equipment package manufactured by Malvern Instruments from the United Kingdom primarily worked as a test device for zeta potential analysis. Particle dispersions were first diluted with a filtered deionized water for analysis to avoid multiple scattering and to increase the counting rate. Gentle sonication of samples for one or two minutes minimized gathering without affecting the intended texture of the surface. The experiment was designed to be run under a constant temperature of 25 degrees Celsius, with precision in temperature within 0.5 degrees Celsius. Every sample had three measurements carried out to confirm their repeatability within the tests[13].

Fourier Transform Infrared Spectroscopy (FTIR)

FTIR spectroscopy was conducted to evaluate whether the drug and polymer materials used in their study could form compatible bonds or react with each other. The Bruker Alpha II FTIR spectrometer from Bruker Optik GmbH Germany with its ATR attachment was used to collect spectra of the drug and polymer materials as well their physical mixture and drug-loaded polymeric nanoparticles[14].

The physical mixture was prepared the by combining the drug and polymer materials according to the same proportions used in their formulation. Each sample was placed directly onto the ATR crystal to measure spectra from 4000 to 400 cm^{-1} while using a 4 cm^{-1} resolution and 32 scan method for each sample. The researchers obtained a background spectrum which they used to establish a reference point for their following measurements.

A comparison was made between the characteristic peaks of the drug and polymer materials with the peaks of both the physical mixture and nanoparticles to detect any shifts or disappearance or broadening of bands which would suggest intermolecular interactions[15].

Differential Scanning Calorimetry (DSC)

While the correct analysis method used in the studies was DSC, the studied thermal behaviour considered the comparison between pure drug, polymer, simple physical mixture, and nanoparticles loaded with the drug. The instrument employed was a calibrated DSC (e.g., TA Instruments DSC Q20), with indium used for calibration as well with enthalpy.

What was done was to weigh accurately, 3–5 mg, samples of pure drug, polymer, simple physical mixture (1:1 w/w), and lyophilized nanoparticles, which were subjected to heat by using an aluminium pan sealed with its empty counterpart as a reference. The heating was done in the range from 25°C to 300°C at a rate of 10°C/min using a 50 mL/min nitrogen purge[16].

From the thermograms, the Tm (melting temperature) and Tg (glass transition temperature), the most characteristic thermal transitions, which were used as informative indices, exhibited disappearance or down varying intensity in such structure peaks. The host matrix or amorphous nature or molecular distribution of the proposed drug nanoparticles is ascertained by the weakening or disappearance of the drug-melting peaks in comparison with the pure drug and simple physical mixture[17].

Entrapment Efficiency and Drug Loading Capacity

Encapsulation efficiency (EE%) and drug loading (DL%) were determined as percentages using the indirect method by measuring unencapsulated drug in

the supernatant. Ultracentrifugation at ultrahigh speed (15,000–20,000 rpm, 30–45 min, 4°C) was then carried out with the aim of completely separating free drug from a solid matrix of nanoparticles; the supernatant was carefully decanted and analyzed with UV–visible spectrophotometry or HPLC analysis for drug characteristics. Finally, the two parameters were obtained by calculation: the amounts of free drug were subtracted from their total initial amounts.

$$\text{EE (\%)} = \frac{\text{Total drug} - \text{Free drug}}{\text{Total Drug}} \times 100$$

$$\text{DL (\%)} = \frac{\text{Total drug} - \text{Free drug}}{\text{Total nanoparticle weight}} \times 100$$

Measurements were performed in triplicates, and data were given in terms of the mean ± standard deviation[18].

***In Vitro* Release of Octenidoine Dihydrochloride Nanoparticles**

In vitro drug release from drug-loaded polymeric nanoparticles was done through the means of the dialysis bag diffusion technique. The nanoparticles, in a quantity that had been accurately weighted to represent a known mass of the drug, were dispersed in 2–5 ml of states of new medium and transferred into pre-washed and pre-soaked dialysis membrane (with MWCO of 12–14 kDa). This membrane was tied and maintained in release medium from 50 to 100 mL (E.g., phosphate-buffered saline, pH 7.4) at 37 ± 0.5°C with constant stirring at 100–200 rpm to ensure sink conditions.

A predetermined number of aliquots were withdrawn and replaced with fresh medium at intervals. UV–Visible spectrophotometry or HPLC are validated methods that can operate to analyze the samples. Cumulative drug release in terms of percentage of total drug content and release kinetics using standard mathematical models were calculated[19].

RESULTS & DISCUSSION

Preparation and Optimization of Octenidine Dihydrochloride

The DOE software was utilized to generate eighteen (18) formulations, each varying in polymer (PLGA) amounts and process parameters (homogenizer speed and sonication period). Table 2 presents the particle size, encapsulation efficiency, and drug loading of each formulation.

Table 2: Formulations of Nanoparticle along with Factors and Responses

Run	A: polymer	B: Homogenization speed	C: sonication time	particle size	entrapment efficiency	drug loading
	%	rpm	min	nm	%	%
1	5	10000	5	265.4	68	8.6
2	2.75	10000	3	245.4	75	9.7
3	2.75	10000	7	248.4	76	10.3
4	2.75	20000	3	252.5	70	9.3
5	0.5	10000	5	233.2	82	11.8
6	2.75	15000	5	260.1	72	9.5
7	2.75	15000	5	262.3	71	9.5
8	2.75	15000	5	261.5	74	9.8
9	0.5	15000	3	235.2	78	10.7
10	2.75	15000	5	262.5	73	9.5
11	5	15000	3	281.3	60	8.5
12	5	15000	7	278.5	65	9
13	2.75	15000	5	266.6	68	9
14	5	20000	5	275.4	63	8.8
15	2.75	20000	7	255.3	73	9.4
16	2.75	15000	5	258.4	71	9.6
17	0.5	15000	7	230.3	80	10
18	0.5	20000	5	240.2	79	9.9

It shows the effect of independent variables on dependent response surface data through glass (like contour plots, three-dimensional graphs, predicted actual graphs, and so forth) and by ANOVA model analysis. The independent factor relationships interaction between in determining the response of the two parties in question through the use of response surface analysis and great insights into the 3D response surface plots and 2D contour plots. These statistics

gave the fullest possible illumination of the optimization environment, showed the essential factor-response relationships.

a) **Particle size:** The statistical evaluation of the developed model utilizing Design-Expert software reveals a strong model significance together with model reliability. The high value for the model F-statistic (34.47) states clearly that it represents high significance as it explains a substantial proportion of the variation in the response, and this proportion is observed to be much greater than the remainder. The most interesting piece of this critique is the finding that the associated P-value is < 0.0001, which is to say that the current dataset has very low possibilities of coming into existence by some random noise. The coefficient of determination (R^2 = 0.9749) indicates that 97.49% of the variability in the response is explained by the model, which denotes an excellent model fit. Adjusted value of R^2 (0.9466) has a value quite comparable to R^2, thus asserting that the model does not suffer over fitness and the predictors accommodated are pertinent to the model. The adequate precision value of 20.3266, which is well above the minimum desirable value of 4, indicates an adequate signal-to-noise ratio. The model enables effective design space navigation.

Final Equation in Terms of Coded Factors:

Particle Size= +261.90 + 21.84A + 5.50B - 0.2375C - 2.50AB + 0.5250AC - 0.0500BC - 2.84A^2 - 8.76B^2 - 2.74C^2

It can be concluded from the model that the particle size is appreciably altered by the different formulation and process variables. Among the individual factors, polymer concentration (A) proved highly impactful, with a positive sign suggesting an increase in polymer concentration producing an increase in particle size. The homogenizer speed (B) also brought a soaked positive effect, but it was far less than that of polymer concentration. In contrast, sonication time (C) presents a very slightly adverse effect, where a minor decrease in particle size occurs with an increase in sonication time.

The variable interactions exhibited here were relatively small. The negative term from AB implied that the combined influence of polymer concentration and homogenization speed would push the further reduction of particle size, whereas the positive term AC suggested a slight increase in particle size due to the interaction between polymer concentration and sonication time. The effect of BC interaction was hardly noticeable.

The quadratic coefficients of A^2, B^2, and C^2 are all negative, indicating that the response surface has natural curvature, thus implying the nonlinear relationship between the independent variables and particle size. The effect according to homogenization speed itself (B^2) were actually quite big among these, showing the most prominent curved effect on the response.

Further such observations indicate that polymer concentration was the dominant factor determining the particle size with the homogenization speed and sonication time contributing to it to some extent. The developed polynomial model effectively explained the joint and nonlinear effects of the variables on particle size.

The response surface data in form of images for particle size are presented bellow

Fig 3: Contour Plot 2D of Particle size (AC)

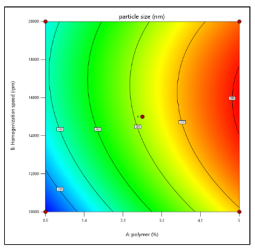

Fig 4: 3D Surface of Particle size (AC)

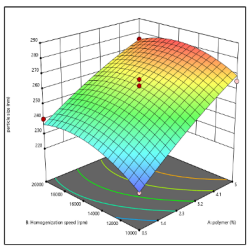

Fig 1: Contour Plot 2D of Particle size (AB)

Fig 2: 3D Surface of Particle size (AB)

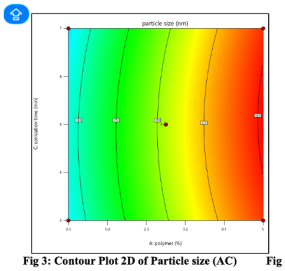

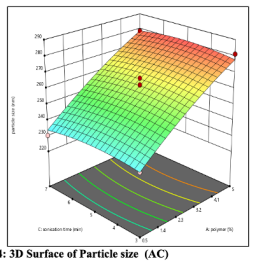

Fig 3: Contour Plot 2D of Particle size (AC)

Fig 4: 3D Surface of Particle size (AC)

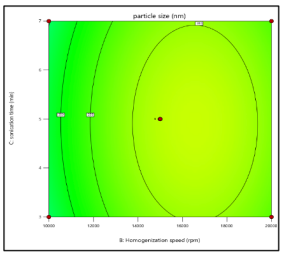

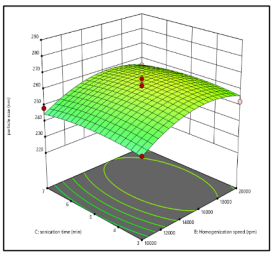

Fig 5: Contour Plot 2D of Particle size (BC)

Fig 6: 3D Surface of Particle size (BC)

b) Entrapment efficiency: The statistical significance of the model here is established by a measurement of 52.24 for F, which further indicates the model['s] making more outcomes than it fails to predict. The p value ($p < 0.0001$) supports the notion that one of the important predictors in the model is unlikely to account for effects that are merely random, N (0, σ^2), and it cannot be brushed off just like this. Determination Coefficient (R^2 = 0.9180), that indicates about 91.80% of casualty variation, the R^2 serving for potential

assessment says that the model, while arriving at good measures, suffers from residuals of explainable 8%.

The model shows no overfitting because its R^2 value matches the Adjusted R^2 value which shows all included variables possess actual significance. The Predicted R^2 value of 0.8682 shows strong forecasting strength because its value only differs from Adjusted R^2 by less than 0.2. The Adequate Precision value of 22.5031 shows a major increase above the required minimum of 4 which proves an acceptable signal-to-noise ratio and validates that the model supports reliable design space navigation.

The Lack of Fit F-value (0.6984) is not significant relative to the pure error, indicating that the lack of fit is insignificant. The model accurately represents the experimental data because it shows no signs of systematic errors.

Final Equation in Terms of Coded Factors:

entrapment efficiency= +72.11 - 7.88A - 2.00B + 1.38C

The model shows that polymer concentration (A) produces the strongest impact on EE because it creates a major negative effect. The research found that higher polymer concentrations decreased entrapment efficiency which indicates that the system experienced either diffusion restrictions or increased viscosity. The research found that homogenization speed (B) created negative effects which were less noticeable than other factors because increased shear conditions caused drug leakage from the formulation.

The research found that sonication time (C) created a positive effect on EE because increasing sonication duration improved drug dispersion and drug incorporation. The coefficient values indicate that polymer concentration represents the main factor which controls entrapment efficiency whereas homogenization speed follows as the second factor and sonication time provides only a small effect.

The research found that optimal conditions which achieved maximum EE required low polymer concentration together with moderate homogenization speed and high sonication time.

The response surface data in form of images for Entrapment efficiency are presented bellow

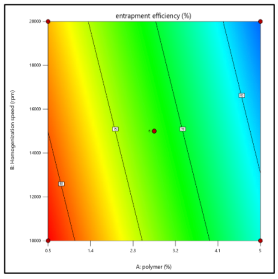

Fig 7: Contour Plot 2D of EE

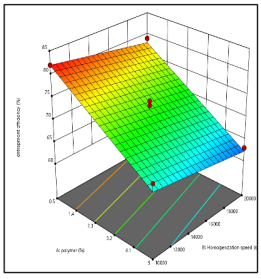

Fig 8: 3D Surface of EE

c) Drug loading capacity: The research team used analysis of variance (ANOVA) to test the statistical significance and the adequacy of their developed model. The regression model achieved highly significant results because its F-value reached 22.80. The result occurs at a P-value smaller than 0.0001 which shows that all model terms reach statistical significance because the likely results from random noise are practically impossible.

The coefficient of determination (R^2 = 0.9256) shows that 92.56% of the response variance gets explained by the model which demonstrates a strong relationship between actual experimental results and the predicted values. The adjusted R^2 value (0.8850) shows close agreement with the R^2 value because the model used relevant terms without creating overfitting. The model shows good predictive ability because the predicted R^2 (0.8211) matches the adjusted R^2 value.

The adequate precision measurement reached 18.5752 which exceeds the required minimum of 4, thus verifying that the model delivers sufficient signal-to-noise performance for effective design space navigation.

The lack-of-fit test produced an F-value of 0.5310 which showed no significant difference when compared to the pure error, thus demonstrating that the lack of fit does not exist. The model demonstrates good fit with experimental data while all systematic errors have been accounted for.

Final Equation in Terms of Coded Factors:

Drug loading = +9.56 - 0.8375A - 0.2750B + 0.0625C + 0.3250AB + 0.3000AC

Drug transport analysis of their nanoparticle makes use of a quadratic model, which has demonstrated how the impact of various formulation and process factors is reflected by the observations. The model showed that the polymer concentration, A, contributed to a significant negative effect on encapsulation efficiency (−0.8375), implying that the higher dispersion of polymer impairs the incorporation of drug. The procedure leads to increased matrix density which prevents drug entrapment efficiency.

Homogenization speed (B) created a negative effect (−0.2750) which showed that higher shear forces cause drug loss during emulsification because drugs diffuse into the external phase.

The controlled sonication process produced a slight positive effect through sonication time (C) which enabled better drug distribution in the polymer matrix and improved loading capacity.

It was found that interaction effects produced positive results because AB (+0.3250) and AC (+0.3000)

showed that polymer concentration combined with process parameters produced synergistic effects. The results indicate that individual factors reduce drug loading but their combined optimization will enhance encapsulation results.

The results show that drug loading depends mainly on polymer concentration which is followed by homogenization speed and sonication time which has a minor role. The drug loading efficiency increases when the variables reach their optimal combination.

The response surface data in form of images for Drug loading capacity are presented bellow

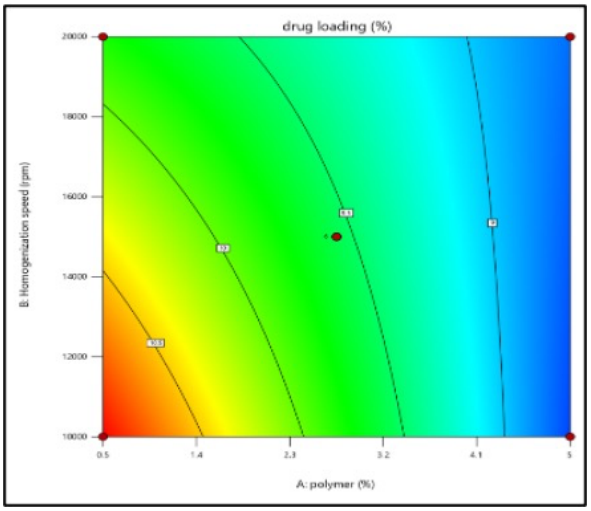

Fig 9: Contour Plot 2D of DL (AB)

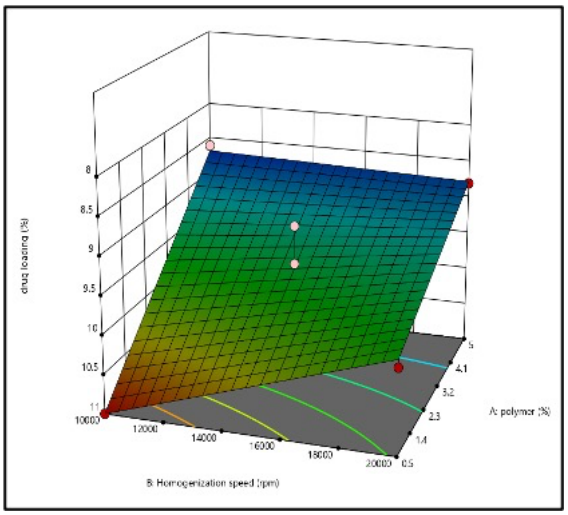

Fig 10: 3D surface of DL (AB)

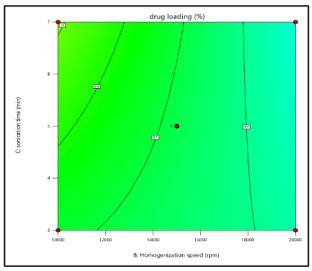

Fig 11: Contour Plot 2D of DL (AC)

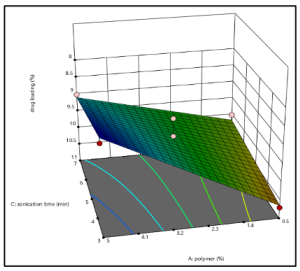

Fig 12: 3D surface of DL (AC)

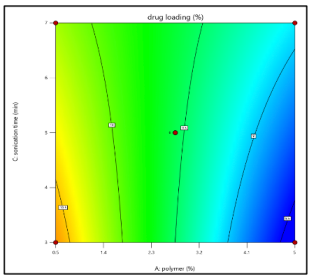

Fig 13: Contour Plot 2D of DL (BC)

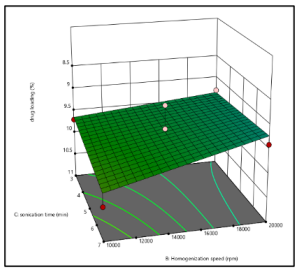

Fig 14: 3D surface of DL (BC)

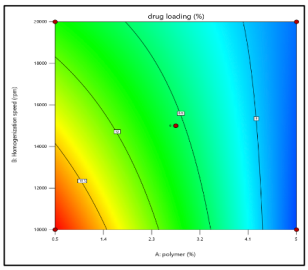

Fig 9: Contour Plot 2D of DL (AB)

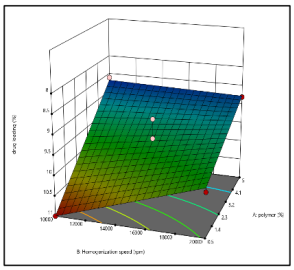

Fig 10: 3D surface of DL (AB)

Characterisation of Octenidoine Dihydrochloride Nanoparticles

Particle Size and PDI

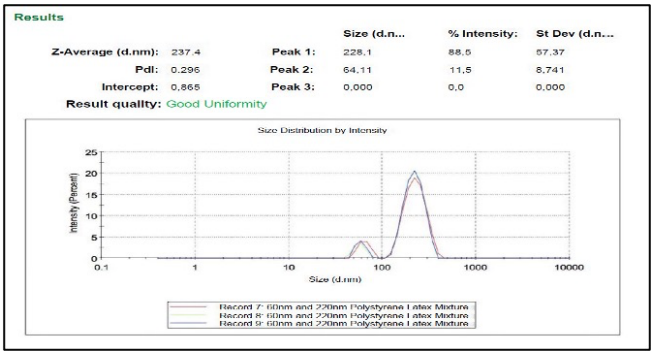

Fig 15: DLS graph indicating Particle size and PDI

Analysis of the Dynamic light scattering study revealed that the average size was 237.4 nm in diameter for the nanoparticles under preparation. The high intensity peak in the particle size distribution profile lies in the nanometre range, indicative of the uniformity of the dispersion of the particles evidenced while only minor aggregations were present.

The calculated value of the Poly Dispersion index (PDI) leads to 0.296 which is quite a low value I and shows an even fair size distribution and homogeneity

that existed among the nanoparticles. Values falling below the 0.3 limit indicate a uniformity present on either part of the formulation and confirm the validity of the preparation procedure.

Particle Charge (Zeta Potential)

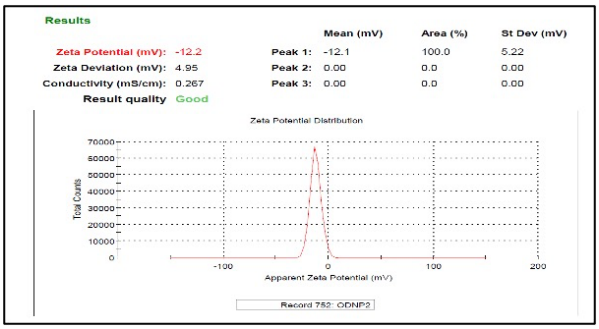

Fig 16: Zeta Potential

These results show that nanoparticles prepared had a zeta potential of -12.2 mV near the neutral point, which had almost the same magnitude an average plus or minus 4.95 mV. In considering the electrophoretic mobility distribution, a peak of almost 100% was visible at -12.1 mV, which signifies that one particle was formed at a given pH with hardly observable secondary particles in the sample. The negative charge observed in the sample leads to moderate colloidal stability; it helps to prevent aggregation due to repulsion created by the negative charge; however, some additional stabilization is strongly recommended since electrostatic repulsion is not enough when referred to larger particles.

Fourier Transform Infrared Spectroscopy (FTIR)

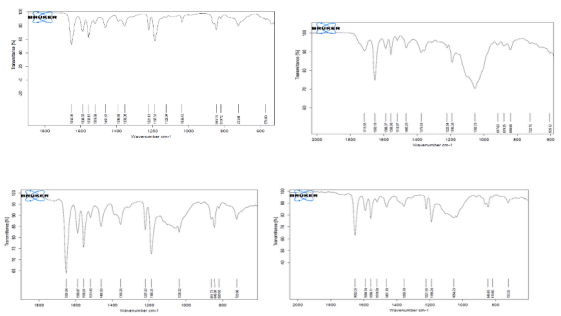

Fig 17: FTIR studies of A. Drug, B. Polymer, C. Physical Mixture of Drug and Polymer, and D. Drug loaded Polymeric nanoparticle

A strong peak was observed at ~1650 cm^{-1}, indicating the C=O stretching of Octonedine dihydrochloride. In addition, there was a significant vibrational region from 1550 to 1590 $cm^{-}1$ probably due to the hydrocarbon ring of octenidine; transmissions above 1200 $cm^{-}1$ finally suggest N—C stretching. This is well indicative that the structure is maintained in either the crystalline or amorphous state.

PLGA showed its typical absorption bands, including a strong peak around 1745 cm^{-1} caused by ester carbonyl (C=O) stretching, on top of peaks near 1180–1090 cm^{-}-1 by C—O—C stretching vibrations.

Physical mixtures showed virtually all the peaks emitted from the two components, and all of these peaks were again well retained on the graph due to the absence of any large shifts in the chemical structure of PLGA by the drug molecules or works of art.

Peak characteristics were preserved in the drug-loaded nanoparticles but with broadening and less intensity for drug peaks, whereas peaks of the species related to polymerized drug were high. The observation of no new peaks and major shifts further imparted that the drug was encapsulated within the PLGA matrix with less concern towards chemical danger between the loaded drug and PLGA.

Differential Scanning Calorimetry (DSC) Studies:

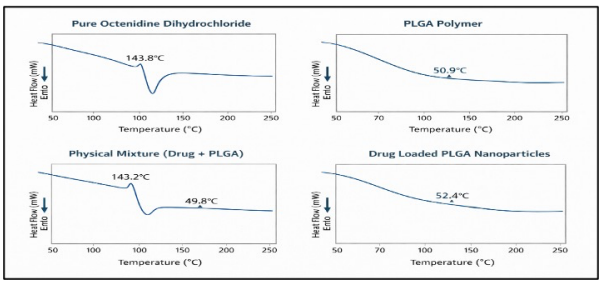

Fig 18: DSC graphs of Drug, polymer, physical mixture drug-polymer and drug loaded nanoparticle

The DSC thermogram of pure Octenidine Dihydrochloride shows a sharp melting peak at 143.8°C, confirming its crystalline nature. PLGA exhibits a glass transition temperature (Tg) around 50.9°C, indicating its amorphous structure.

The physical mixture displays both the drug melting peak (143.2°C) and PLGA Tg (49.8°C), suggesting no significant interaction between them.

In the drug-loaded PLGA nanoparticles, only the Tg at 52.4°C is observed, while the drug's melting peak disappears. This indicates that the drug is present in an amorphous or molecularly dispersed form within the polymer matrix.

Entrapment Efficiency and Drug Loading Capacity

The optimized nanoparticle formulation demonstrated an adequate drug incorporation indicated by its entrapment efficiency and drug loading capacity. Entrapment efficiency was 81.08 ± 1.19% for this formulation, indicating that a large portion of the drug

was successfully encapsulated in the nanoparticulate system.

The formulation exhibited excellent drug loading capacity, 11.99 ± 0.71%, giving it a significant drug present relative to its weight of nanoparticles. This clearly shows that the formulation process has been effective to achieve highly efficient drug encapsulation and a notable drug-loading characteristic.

Table 3: Entrapment Efficiency and Drug Loading Capacity of the optimized batch

Entrapment Efficiency (%)				Drug loading capacity (%)			
Reading I	Reading II	Reading III	Mean ± SD	Reading I	Reading II	Reading III	Mean ± SD
81.43	79.76	82.07	**81.08 ± 1.19**	11.28	12.01	12.69	**11.99 ± 0.71**

***In Vitro* Release of Octenidoine Dihydrochloride Nanoparticles**

Table 4: *In Vitro* Release of Optimized nanoparticle batch

Time (hours)	% Drug Released	Release Mechanism
1	20.2 ± 1.8	Initial burst release due to surface drug.
4	41.59 ± 2.9	Sustained release phase begins.
8	65.7 ± 1.9	Controlled diffusion through polymer matrix.
12	80.5 ± 2.3	Near-linear release kinetics.
24	94.3 ± 2.2	Plateau phase, the majority of the drug is released.

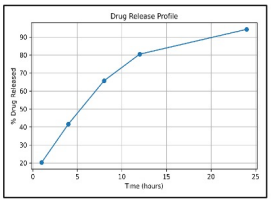

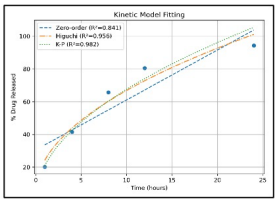

Fig 19: Drug release profile of optimized batch
Fig 20: Kinetic model fitting of optimized batch

The drug release profile displayed a biphasic pattern, first the burst release of 20.2 ± 1.8% at 1 h with the surface-associated drug was followed by a sustained release phase. The cumulative release increased to 65.7 ± 1.9% at 8 h and 80.5 ± 2.3% at 12 h, evidenced the polymer matrix and controlled diffusion. At 94.3 ± 2.2%, cumulation was reduced to zero at 24 h intimation of almost total drug release.

The mathematical model application indicated poor fitness for zero order ($R^2 = 0.841$), but good correlation for Higuchi ($R^2 = 0.956$) suggested diffusion-controlled release. The Korsmeyer–Peppas model showed the best fit with $R^2 = 0.982$ and release exponent ($n = 0.509$), verifying Fickian diffusion as the major mechanism.

At large, the formulation provided controlled and sustained release of the drug, which was mainly operating through diffusion throughout the polymer matrix.

CONCLUSION

In this study, the development of the optimized formulation via Box–Behnken design was successful for developing Octenidine Dihydrochloride -loaded PLGA nanoparticles to undergo a robust and systematic setting. The application of design of experiments propagated accurate resolution of the individual as well as interdependent effects of formulation and process variables, with polymer concentration determined to be getting the thickest say in particle size, drug encapsulation, and loading efficiency. The optimized formulation was made of nanosized particles with relatively narrow dispersity; an acceptable surface charge; high encapsulation efficiency; and impressive drug loading, indicating the predictability and reproducibility of the developed system.

Comprehensive physicochemical characterization highlights the structural integrity and compatibility of the drug–polymer system. Any interference due to chemical interaction was dispelled by FTIR analysis on characteristic functional groups, and DSC studies established the drug's amorphous or molecularly dispersed state within the polymeric matrix. The outcome suggests successful encapsulation and stabilization of Octenidine Dihydrochloride, which is crucial to increasing its formulation efficiency. The relatively low zeta potential and mono-distilled nanoparticles it demonstrates by means of DLS strengthens the argument for a stable colloidal system for biomedical applications.

The bi-phasic pattern seen in the in-vitro release studies showed the initial burst-like release of ibrutinib followed by steady-state drug release over 24h that suits in accordance with the therapeutic requirements of a wound dressing. According to kinetic modelling, drug release mainly follows a diffusion-controlled mechanism correlated well (R=0.9971) with the Higuchi and Korsmeyer-Peppas models. This release will provide an edge in terms of reused antibacterial activity at a wound site, lessening the frequency of drug administration and thereby enhancing the therapeutic effectiveness.

This article introduces an initiative to modify these drug delivery systems for more beneficial types of use within the ambit of advanced wound care concepts. The various positive features such as proper physicochemical properties, suitability for loading drugs, and controlled release make this platform highly profitable for further translational research. Multifunctional hydrogel matrices might enhance the future work of the project, bearing validation for the usability of the system in an actual clinical setting to bring the potential to be a next generation wound dressing technology.

ACKNOWLEDGEMENTS

The authors are grateful to the laboratory staff for technical assistance during this study.

CONFLICT OF INTEREST

There is no conflict of interest to authors in publication

REFERENCE

1. Singh, A. R., & Athawale, R. B. (2023). Revolutionizing Drug Delivery: The Potential of PLGA Nanoparticles in Nanomedicine. *Current Applied Polymer Science*, *6*(2), 87–100. https://doi.org/10.2174/0124522716282353240118114732
2. Narmani, A., Jahedi, R., Bakhshian-Dehkordi, E., Ganji, S., Nemati, M., Ghahramani-Asl, R., Moloudi, K., Hosseini, S. M., Bagheri, H., Kesharwani, P., Khani, A., Farhood, B., & Sahebkar, A. (2023). Biomedical applications of PLGA nanoparticles in nanomedicine: Advances in drug delivery systems and cancer therapy. *Expert Opinion on Drug Delivery*, *ahead-of-print*(ahead-of-print), 937–954. https://doi.org/10.1080/17425247.2023.2223941
3. Karpiński TM, Korbecka-Paczkowska M, Zeidler A, Grzywna W. Octenidine Dihydrochloride – Antimicrobial Activity, Adaptation and Clinical Application. Advancements Microbiol. 2025;64(3):182–191. https://doi.org/10.2478/am-2025-0014
4. Bakrey, H., Abdu, A., Shivgotra, R., Soni, B., Sharma, M., Bakrey, A., & Jain, S. K. (2025). Innovative Strategies and Advances in Drug Delivery Systems to Address Poor Solubility: A Comprehensive Review. *Current Drug Targets*, *26*(13), 879–902. https://doi.org/10.2174/0113894501375776250713110838
5. Maraldi, M., Guida, A., Sponchioni, M., & Moscatelli, D. (2020). Influence of the Polymer Architecture and Functionalization with Carboxylate Groups over the Release of Octenidine Hydrochloride from Poly(lactic acid)-Based Nanoparticles. *Macromolecular Materials and Engineering*, *306*(2), 2000592. https://doi.org/10.1002/mame.202000592
6. Gaspar, L. M. D. A. C., Dórea, A. C. S., Droppa-Almeida, D., De Mélo Silva, I. S., Montoro, F. E., Alves, L. L., Macedo, M. L. H., & Padilha, F. F. (2018). Development and characterization of PLGA nanoparticles containing antibiotics. *Journal of Nanoparticle Research*, *20*(11). https://doi.org/10.1007/s11051-018-4387-z
7. Banker, G. S. (2019). *Pharmaceutical Applications of Controlled Release: An Overview of the Past, Present, and Future* (pp. 1–34). Crc. https://doi.org/10.1201/9780429276620-1
8. Cai, X., Jin, M., Yao, L., He, B., Ahmed, S., Safdar, W., Ahmad, I., Cheng, D.-B., Lei, Z., & Sun, T. (2023). Physicochemical properties, pharmacokinetics, toxicology and application of nanocarriers. *Journal of Materials Chemistry B*, *11*(4), 716–733. https://doi.org/10.1039/d2tb02001g
9. Supraba, W., Husni, P., Hazrina, A., Kusuma Dewi, M., & Yohana Chaerunisaa, A. (2025). Challenges and Strategies in Nanoparticle-Mediated Drug Release: Mechanisms and Future Directions. *Trends in Sciences*, *22*(10), 10344. https://doi.org/10.48048/tis.2025.10344
10. D'Ambrosio, A., Scialla, S., Piemonte, V., Moscatelli, D., & Mauri, E. (2025). Drug Delivery from Nanogel Formulations: Mathematical Modeling of Different Release Profiles and Conditions. *Molecular Pharmaceutics*, *22*(11), 6611–6622. https://doi.org/10.1021/acs.molpharmaceut.5c00494
11. Fernández-Carballido A, Puebla P, Herrero-Vanrell R, Pastoriza P. Radiosterilisation of indomethacin PLGA/PEG-derivative microspheres: Protective effects of low temperature during gamma-irradiation. Int J Pharm. 2006;313(1–2):129–135. https://doi.org/10.1016/j.ijpharm.2006.01.039
12. Torquato LM, Hélaine N, Cui Y, O'Connell R, Gummel J, Robles ESJ, et al. Microfluidic in-line dynamic light scattering with a commercial fibre optic system. Lab Chip. 2023;23(11):2540–2552. https://doi.org/10.1039/d3lc00062
13. Das SK, Chakraborty S, Rajabalaya R, Mazumder B. Zeta potential measurements and analysis for biomedical nanotechnology. 2023:17. https://doi.org/10.1088/978-0-7503-3379-5ch17
14. Fahelelbom KM, Saleh A, Al-Tabakha MMA, Ashames AA. Recent applications of quantitative analytical FTIR spectroscopy in pharmaceutical, biomedical, and clinical fields: A brief review. Rev Anal Chem. 2022;41(1):21–33. https://doi.org/10.1515/revac-2022-0030
15. Song Y, Cong Y, Wang B, Zhang N. Applications of Fourier transform infrared spectroscopy to pharmaceutical preparations. Expert Opin Drug Deliv. 2020;17(4):551–571. https://doi.org/10.1080/17425247.2020.1737671
16. Groël S, Menzen T, Winter G. Calorimetric Investigation of the Relaxation Phenomena in

Amorphous Lyophilized Solids. Pharmaceutics. 2021;13(10):1735. https://doi.org/10.3390/pharmaceutics13101735

17. Thun J, Martin N. Standards and Trends in Solid-State Characterization Techniques – Thermal Analysis. 2021:129–149. https://doi.org/10.1002/9783527823048.ch4-3
18. Patle MB, Dhapake PR. Introduction to Nanoparticles in Pharmacy: A Review. Asian J Res Pharm Sci. 2024;367–372. https://doi.org/10.52711/2231-5659.2024.00058
19. Paraskevopoulou V, Mead H, Gibson R, Amerio-Cox M, Taylor-Vine G, Mann J. Developing a Robust In Vitro Release Method for a Polymeric Nanoparticle: Challenges and Learnings. Br J Pharm. 2023;8(2). https://doi.org/10.5920/bjpharm.1358